International Journal of Heat and Mass Transfer 111 (2017) 321–328

Contents lists available at ScienceDirect

International Journal of Heat and Mass Transfer

journal homepage: www.elsevier.com/locate/ijhmt

On the discontinuity of the dissipation rate associated with the temperature variance at the fluid-solid interface for cases with conjugate heat transfer

Flageul Cédric [a,b,*], Benhamadouche Sofiane [b], Lamballais Éric [c], Laurence Dominique [d,b]

[a] Institut Jožef Stefan, R4 Division, Jamova cesta 39, SI-1000 Ljubljana, Slovenia
[b] EDF R&D, Fluid Mechanics, Energy and Environment Dept., 6 Quai Wattier, 78401 Chatou, France
[c] Institute PPRIME, Department of Fluid Flow, Heat Transfer and Combustion, Université de Poitiers, CNRS, ENSMA, Téléport 2 - Bd. Marie et Pierre Curie, B.P. 30179, 86962 Futuroscope Chasseneuil Cedex, France
[d] School of Mechanical, Aerospace and Civil Engineering, The University of Manchester, Sackville Street, Manchester M13 9PL, UK

ARTICLE INFO

Article history:
Received 18 October 2016
Received in revised form 25 March 2017
Accepted 3 April 2017

Keywords:
Conjugate heat transfer
Dissipation rate
RANS
Direct Numerical Simulation
Turbulent channel flow

ABSTRACT

In the case of conjugate heat transfer, the dissipation rate associated with the temperature variance is discontinuous at the fluid-solid interface. The discontinuity satisfies a compatibility condition involving the fluid-solid thermal diffusivity and conductivity ratios and the relative contribution to the dissipation rate of its wall-normal part. The present analysis is supported by the Direct Numerical Simulations of an incompressible channel flow at a Reynolds number, based on the friction velocity, of 150, a Prandtl number of 0.71 and several values of fluid-solid thermal diffusivity and conductivity ratios.

1. Introduction

Conjugate heat transfer describes the thermal coupling between a fluid and a solid. It is of prime importance in industrial applications where fluctuating thermal stresses are a concern, e.g. in case of a severe emergency cooling or long-term ageing of materials. For such complex applications, investigations often rely on experiments, high Reynolds RANS (Reynolds-averaged Navier-Stokes) or wall-modelled LES (Large Eddy Simulation). However, experimental data on conjugate heat transfer are scarce. Walls in lab rigs are often made of plexiglas and the transported scalar studied is often a dye. These common experimental configurations cannot be used to study conjugate heat-transfer as the dye does not penetrate into the wall. Analytical analysis and DNS (Direct Numerical Simulation) are valuable tools for understanding the flow physics of such complex phenomena and providing reliable data in order to improve RANS and LES modelling.

Numerical study on conjugate heat transfer started with the 2D synthetic turbulence study of Kasagi et al. [1]. Some experimental and analytical studies have been performed prior to this study, in particular Polyakov [2] and Geshev [3], as documented by [1]. The first DNS with conjugate heat transfer was a turbulent channel flow, performed by Tiselj et al. [4]. Following those studies, the authors [5] have also performed DNS of the turbulent channel flow with conjugate heat transfer, with a post-processing designed to produce validation data for RANS models.

The development of RANS approaches for conjugate heat transfer is relatively recent and was pioneered by Craft et al. [6]. In order to allow an accurate estimation of the fatigue, (U)RANS models adapted to conjugate heat transfer should enable the simulation of at least a few minutes of operation in realistic conditions, in order to include as much high stress amplitude events as possible, knowing they generally are low probability events [7].

The structure of the paper is as follows. In the second section, it is established that in case of conjugate heat transfer, the dissipation rate associated with the temperature variance is discontinuous at the fluid-solid interface. This discontinuity satisfies a compatibility condition involving the fluid-solid thermal diffusivity and conductivity ratios and the relative contribution to the dissipation rate of its wall-normal part. In the third section, the case and numerical setup are described: 9 DNS of incompressible channel flow with conjugate heat transfer are presented. In the fourth section, the corresponding results are presented and the discontinuity of the dissipation rate ε_θ at the fluid-solid interface is high-

* Corresponding author at: Institut Jožef Stefan, R4 Division, Jamova cesta 39, SI-1000 Ljubljana, Slovenia.
E-mail address: cedric.flageul@ijs.si (F. Cédric).

http://dx.doi.org/10.1016/j.ijheatmasstransfer.2017.04.005
0017-9310/

lighted. In the fifth section, our results are further discussed alongside with the consequences for RANS and LES modelling.

2. Governing equations and discontinuity of ε_θ

In the fluid domain (Ω_f), the mass and momentum equations read:

$$\partial_i u_i = 0$$
$$\partial_t u_i = -\frac{\partial_j(u_i u_j) + u_j \partial_j u_i}{2} - \frac{\partial_i p}{\rho} + \nu \partial_{jj} u_i + f_i \tag{1}$$

where ρ is the density, ν is the kinematic viscosity, the convective term is expressed using the skew-symmetric formulation and f_i is a source term.

In case of conjugate heat transfer, the energy equations read:

$$\begin{aligned}
&\partial_t T_f = -\partial_j(T_f u_j) + \alpha_f \partial_{jj} T_f + f_{T_f} \text{ in } \Omega_f \\
&\partial_t T_s = \alpha_s \partial_{jj} T_s + f_{T_s} \text{ in } \Omega_s \\
&T_f = T_s \text{ on } \partial\Omega_f \cap \partial\Omega_s \\
&\lambda_f \partial_n T_f = \lambda_s \partial_n T_s \text{ on } \partial\Omega_f \cap \partial\Omega_s
\end{aligned} \tag{2}$$

where Ω_f (Ω_s), T_f (T_s), α_f (α_s) and λ_f (λ_s) are the fluid (solid) domain, temperature, thermal diffusivity and thermal conductivity, respectively, f_{T_f} and f_{T_s} are source terms and $\partial_n T = \nabla(T)\cdot\mathbf{n}$ is the wall-normal derivative of the temperature with $\mathbf{n}$ a unit vector normal to the fluid-solid interface surface ($\partial\Omega_f \cap \partial\Omega_s$), ∇ being the gradient operator. The last 2 lines in Eq. (2) express the continuity of temperature and heat flux at the fluid-solid interface.

Within this context, the dissipation rate $\varepsilon_{\theta f}$ ($\varepsilon_{\theta s}$) associated with the temperature variance in the fluid (solid) domain can be defined:

$$\begin{aligned}
&\varepsilon_{\theta f} = 2\alpha_f \overline{\nabla\left(T_f'\right)\cdot\nabla\left(T_f'\right)} \text{ in } \Omega_f \\
&\varepsilon_{\theta s} = 2\alpha_s \overline{\nabla\left(T_s'\right)\cdot\nabla\left(T_s'\right)} \text{ in } \Omega_s
\end{aligned} \tag{3}$$

where T' and the overline are the fluctuating part of the temperature T and the averaging operator, respectively. Using the continuity of temperature and heat flux at the fluid-solid interface, it is straightforward to show that the dissipation rates satisfy the following relation:

$$\begin{aligned}
\frac{\varepsilon_{\theta f}}{2\alpha_f} - \frac{\varepsilon_{\theta s}}{2\alpha_s} &= \overline{\partial_n T_f' \partial_n T_f'} - \overline{\partial_n T_s' \partial_n T_s'} \quad \text{on} \quad \partial\Omega_f \cap \partial\Omega_s \\
&= \overline{\partial_n T_f' \partial_n T_f'}\left[1 - \left(\frac{\lambda_f}{\lambda_s}\right)^2\right] \quad \text{on} \quad \partial\Omega_f \cap \partial\Omega_s
\end{aligned} \tag{4}$$

Using the thermal properties α and λ, dimensionless numbers can be derived. Following Flageul et al. [5], one defines G as the fluid-to-solid thermal diffusivity ratio and G_2 as the solid-to-fluid thermal conductivity ratio:

$$G = \frac{\alpha_f}{\alpha_s}, \quad G_2 = \frac{\lambda_s}{\lambda_f} \tag{5}$$

Combining G and G_2, one may obtain the thermal activity ratio K ($\frac{1}{K} = G_2\sqrt{G}$) as defined by Geshev [3] and Tiselj et al. [4], which is also the fluid-to-solid thermal effusivity ratio. On this basis, Eq. (4), combined with the definition of $\varepsilon_{\theta f}$ in Eq. (3) turns to:

$$\begin{aligned}
&1 - G\frac{\varepsilon_{\theta s}}{\varepsilon_{\theta f}} = \frac{\overline{\partial_n T_f' \partial_n T_f'}}{\overline{\nabla T_f'\cdot\nabla T_f'}}\left[1 - \frac{1}{G_2^2}\right] \\
&\iff \frac{1}{G} - \frac{\varepsilon_{\theta s}}{\varepsilon_{\theta f}} = \frac{\overline{\partial_n T_f' \partial_n T_f'}}{\overline{\nabla T_f'\cdot\nabla T_f'}}\left[\frac{1}{G} - K^2\right] \\
&\iff \frac{\varepsilon_{\theta s}}{\varepsilon_{\theta f}} = \frac{\overline{\partial_n T_f' \partial_n T_f'}}{\overline{\nabla T_f'\cdot\nabla T_f'}}K^2 + \left(1 - \frac{\overline{\partial_n T_f' \partial_n T_f'}}{\overline{\nabla T_f'\cdot\nabla T_f'}}\right)\frac{1}{G}
\end{aligned} \tag{6}$$

It is important to stress that $\mathbf{n}$ is locally well-defined as long as the fluid-solid interface surface is flat or curved but becomes ill-defined for instance at the edge of a corner. Therefore, in case of conjugate heat transfer, the dissipation rate ε_θ at the fluid-solid interface satisfies the compatibility condition (6) for any smooth interface.

In the following, any ratio $\frac{\varepsilon_{\theta s}}{\varepsilon_{\theta f}} \neq 1$ corresponds to a discontinuity of the dissipation rate ε_θ across the fluid-solid interface. It is important to stress that the relative contribution of the wall-normal part in $\varepsilon_{\theta f}$ is bounded in $[0, 1]$. Therefore, Eq. (6) is a convex combination between $\frac{1}{G}$ and K^2.

On the one hand, if the conjugate case is close to an imposed temperature one (conducting solid, $G_2 \gg 1$), then the wall-normal contribution in $\varepsilon_{\theta f}$ dominates at the interface and the discontinuity scales with the squared thermal activity ratio K. On the other, if the conjugate case is close to an imposed heat flux one (insulating solid, $G_2 \ll 1$), then the wall-parallel contribution in $\varepsilon_{\theta f}$ dominates at the interface and the discontinuity scales with the inverse of the thermal diffusivity ratio G. For the other cases, the discontinuity is bounded by $\frac{1}{G}$ and K^2. This range may be quite extended, for instance, considering pressurized water as the fluid and steel as the solid, approximate values are $K^2 \approx 0.01$ and $1/G \approx 60$.

3. Case and numerical setup

Present simulations are based on the open-source software Incompact3d developed at Université de Poitiers and Imperial College London by Laizet et al. [8,9]. Sixth-order compact schemes are used on a Cartesian grid stretched in the wall-normal direction. The pressure is computed with a direct solver on a staggered grid while velocity components and temperature are collocated.

In the present study, x, y and z stand for the streamwise, wall-normal and spanwise directions, respectively, as sketched in Fig. 1. Periodic boundary conditions are used in the streamwise and spanwise directions. The source term driving the channel flow is present only in the streamwise direction: it is a constant in space and time fitted so that the averaged bulk velocity is 1. This source term physically represents the mean pressure gradient compensating the viscous friction at the wall in order to reach a statistically steady state. The channel half-height is also 1, and the Reynolds number based on those quantities is 2280, while the Prandtl number is 0.71 and the density is 1.

The main simulation parameters are recalled in Table 1 and compared with reference ones [10,4]. As described in Flageul et al. [5], the scalar diffusion scheme used is 4th order accurate in the streamwise direction and 6th order accurate in the others. Compared to the simulation from Kasagi et al. [10], our domain is 63 % longer, 35 % wider while we use cells of a similar size. In addition, the duration of our simulation is almost 14 times longer while our time step is 6 times smaller. This point is further dis-

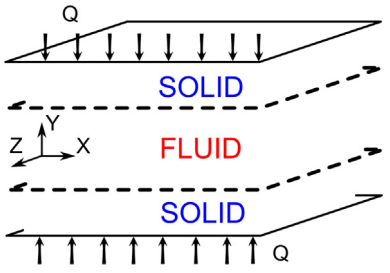

Fig. 1. Sketch of the computational domain.